

**Relative infaunal bivalve  
density assessed from  
split beam echosounder  
angular information**

doi:10.5697/oc.56-3.497  
**OCEANOLOGIA**, 56 (3), 2014.  
pp. 497–521.

© *Copyright by*  
*Polish Academy of Sciences,*  
*Institute of Oceanology,*  
2014.

**KEYWORDS**

Shellfish beds  
Stock assessment  
Split-beam echosounder  
Angular information  
Haralick textural features  
Benthic habitat mapping

NOELA SÁNCHEZ-CARNERO<sup>1,\*</sup>  
DANIEL RODRÍGUEZ-PÉREZ<sup>2</sup>  
NURIA ZARAGOZÁ<sup>3</sup>  
VICTOR ESPINOSA<sup>3</sup>  
JUAN FREIRE<sup>4,5</sup>

<sup>1</sup> Grupo de Oceanografía Física,  
Universidade de Vigo,  
Campus Lagoas-Marcosende, 36200 Vigo, Spain;  
e-mail: noelas@gmail.com

\*corresponding author

<sup>2</sup> Departamento de Física Matemática y de Fluidos,  
Facultad de Ciencias, UNED,  
C/Paseo de la Senda del Rey, 28040 Madrid, Spain

<sup>3</sup> Institut d'Investigació per a la Gestió Integrada de Zones Costaneres,  
C/Paranimf 1, 46730 Grau de Gandia, Spain

<sup>4</sup> Barrabés Next,  
C. Serrano 16-1, 28001 Madrid, Spain

<sup>5</sup> Teamlabs,  
C. Gobernador 26, 28014 Madrid, Spain

Received 30 April 2013, revised 30 January 2014, accepted 4 March 2014.

The complete text of the paper is available at <http://www.iopan.gda.pl/oceanologia/>

**Abstract**

Management of shellfish resources requires a spatial approach where mapping is a key tool. Acoustic techniques have been rarely used to map infaunal organisms with a patchy distribution. We propose and test the use of split-beam echosounder angular information to assess razor shell presence and relative density. Our statistical approach combines textural analysis of angular echograms, standard unsupervised multivariate methods and hierarchical classification through dendrograms to identify groups of locations with similar clam densities. The statistical analyses show that the classification is consistent with groundtruthing data and that results are insensitive to boat motion or seabed granulometry. The method developed here constitutes a promising tool for assessing the relative density of razor clam grounds.

**1. Introduction**

Several marine invertebrate species have been over-exploited throughout the world and, in some instances, depleted (Jamieson 1993, Jamieson & Campbell 1998). During the past 10 years most of the sustainable management strategies aiming to avoid over-exploitation have used spatial regulations such as rotations, marine protected areas (MPA) or territorial use rights. These strategies and their information needs have increased research efforts to develop reliable methods for mapping species and habitats to both understand and classify marine habitats and to manage fishing effort in order to increase the sustainability and/or the yield of fisheries (Kostylev et al. 2003, Adams et al. 2010, Schimel et al. 2010).

In the case of benthic species, the traditional sampling methods (e.g. in situ techniques such as scuba diving, corers and dredges) used for mapping have limited coverage and a high cost in terms of time and money. There is therefore a need for a methodology that could provide data abundance of these benthic species accurately and cost-effectively (Grizzle et al. 2005).

Acoustic methods are the most efficient for the mapping and monitoring of large benthic areas (Anderson et al. 2008), and a low-cost alternative to direct sampling for mollusc reefs (DeAlteris 1988, Wildish et al. 1998, Allen et al. 2005, Grizzle et al. 2005, Hutin et al. 2005, Lindenbaum et al. 2008, Snellen et al. 2008, JiangPing et al. 2009, Raineault et al. 2011). However, no similar method has been developed for infaunal mollusc populations such as razor clams.

Atlantic razor clams inhabit intertidal and subtidal sandy bottoms because oxygen can diffuse through them, which is not the case with muddy bottoms. These solenids can dig down to depths of 60 cm. A habitat preference for sandy bottoms with finer granulometry has been observed, although this has been related to larval settlement (Holme 1954, Darriba

Couñago & Fernández Tajés 2011), and thus does not affect their distribution in seeded beds. Furthermore, as razor clams are not sensitive to sand composition or grain shape, their presence has to be detected independently of the different acoustic responses caused by the different types of sediments.

The acoustic response from the ocean bottom has two components: scattering from the rough water-sediment interface and volume backscattering. The former is caused by the impedance contrast between sediment and water, whereas the latter originates from sediment grains, shell debris and infaunal species. Both contributions are so mixed that it is difficult to characterise the sediment structure using this information (Diaz et al. 2004, Anderson et al. 2008). It is generally assumed that for high-frequency echosounders (i.e.  $f \geq 100$  kHz) the backscattered energy originates mostly in the water-sediment interface (because of the high attenuation of the compressional waves in the sediment). However, when shell hash is present in the volume, its scattering may dominate above the critical (grazing) angle for frequencies just above 60 kHz (Lyons 2005).

The acoustic signal returning to an echosounder contains not only power but also phase information from the wavefront. Measurement of phase differences at different parts of the transducer allows point-like scatterers to be located: the phase difference is related to the angle formed by the scatterer's line of sight and the acoustic beam axis. This is actually the principle behind split-beam echosounders (Foote 1986, Bodholt et al. 1989, Simmonds & MacLennan 2005). The first commercial split-beam echosounder was introduced in 1984 and took advantage of new electronic technologies and developments in acoustic signal processing (Foote et al. 1984). The transducer of a split-beam echosounder is usually divided into four quadrants, which allow the measurement of angles in the athwartship and alongship directions. Individual fishes can be tracked and, through continuous insonification, their direction and speed of motion can be assessed (Arrhenius et al. 2000, Peirson & Frear 2003, Boswell et al. 2007). These angular measurements (or phase differences) also provide information about objects protruding from the seabed. Angular information has been applied to the acoustic 3D imaging of the deep sea-floor (see Cutter & Demer 2010 and the references therein).

Our objective here is to present a method for discriminating between surface and volume components in the acoustic signal in order to detect the presence and relative density of razor clams within the seabed. The challenge is to use the angular information provided by a split-beam echosounder in shallow waters to extract the relevant statistical features for discriminating among high-density, low-density and depleted razor clam beds.

The article is organised as follows. In section 2, the study area, groundtruthing stations and sampling methodology in the acoustic survey are described. In section 3, the statistical methods used to analyse the split-beam angular information are presented in detail. Section 4 presents the results obtained with the statistical unsupervised classification. In section 5, these results are discussed regarding their statistical significance and the potential effects that other experimental and environmental factors could have on them. Section 6 presents the main conclusions of the work.

## 2. Material and experimental methods

### 2.1. Study area

The study was carried out in the Ría de Pontevedra (Galicia, NW Spain), an area fished by ten fishermen's associations that harvest fish, crustaceans and molluscs (bivalves and cephalopods).

One of the most economically important molluscs in this area is the razor clam, which includes three different species: *Ensis ensis*, *E. siliqua* and *Solen marginatus*. All of them are infaunal bivalves with an elongated and semi-rectangular shape, usually found in high-density patches (beds), surrounded by very low density areas.

The fishermen of Ría de Pontevedra harvest 46 different razor clam beds characterised by continuous sandy areas with a homogeneous mollusc density. These areas are distributed between 0 and 12 m below the sea surface, with an average size of  $11.76 \times 10^4 \text{ m}^2$  (Fismare 2011). Three of these razor clam beds, regularly exploited by fishermen, were considered for this study: Raxó, Aguete and A Cova (Figure 1). These three beds are located in sandbars 5–11 m deep and have approximate areas of 9.3, 6.7 and  $28.3 \times 10^4 \text{ m}^2$  respectively. Based on the razor clam harvesting density, the areas were qualitatively described as very productive (Raxó), productive (Aguete) or non-productive (A Cova) by local fishermen at the time of the survey; we hypothesised that productivity is directly related to density.

### 2.2. Groundtruthing stations

Six sampling points, two per sandbar (see Figure 3, p. 507), were set up to measure the actual density of razor clams and other (epibenthic) bivalves, and the granulometric characteristics of the seabed. The biological communities were characterised using a suction pump with a net retaining individuals larger than 1 cm in size. The number of individuals of razor clams and other bivalves were counted at each sampling station and the density was estimated using the area of the sampling frame. Sediment samples were collected with a 30 cm corer. Then they were dried in an oven at

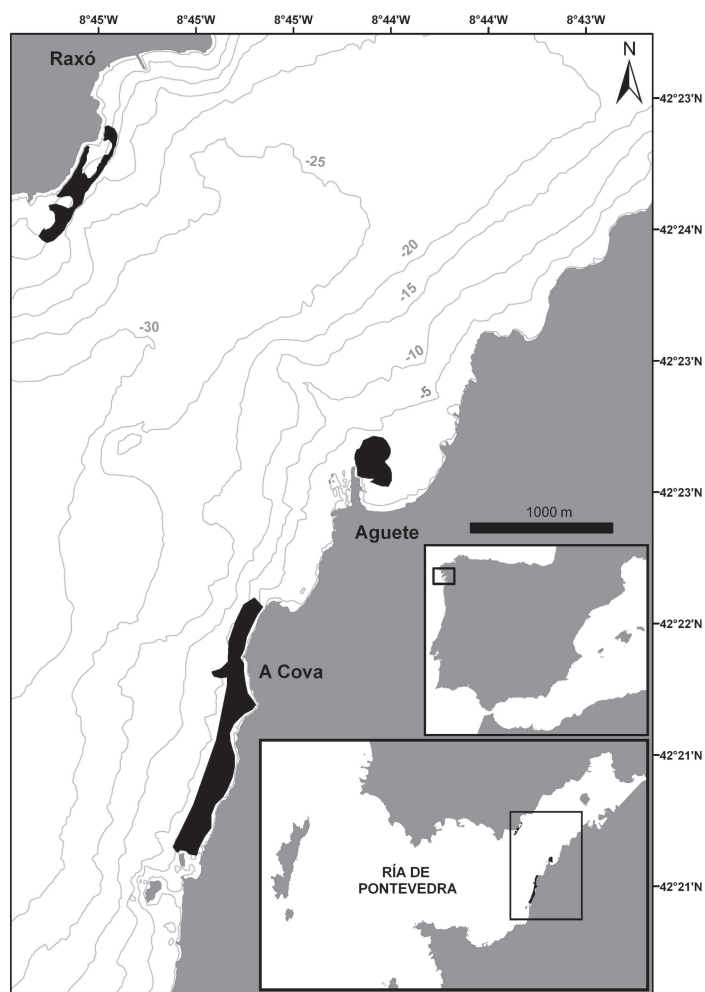


**Figure 1.** Study area in the Ría de Pontevedra; the clam beds under study are highlighted

80°C for two days and apportioned using a 1000  $\mu\text{m}$  analytical sieve (Retsch, Düsseldorf, Germany). Their size distribution was estimated with a laser granulometer (LS200, Beckman Coulter Inc, Brea, CA, USA) and classified according to the Folk classification (Folk 1954, Jackson & Richardson 2007). All this information is summarised in Table 1.

### 2.3. Acoustic survey

The acoustic survey was carried out on 12 July 2009, using a small fishing boat (6.25 m long). A Simrad EK60 scientific echosounder with an

**Table 1.** Groundtruthing data and harvesting information provided by local fishermen for the three razor clam beds. The last four columns show the clusters in Figures 5 and 6 (see pp. 509–510) with their elements (transect segments) geographically closer to these stations; the asterisks denote those clusters with mixed segments

Bank	Station	Depth [m]	Sand granulometry (Folk classification)	Razor clam density [indiv. m <sup>-2</sup> ]	Other infaunal bivalves [indiv. m <sup>-2</sup> ]	Type 1 Port	Type 1 Starboard	Type 2 Port	Type 2 Starboard
Raxó	1	5.4	medium-fine	high (124)	112	b2	a*	b1	b2_2
	2	6.4	medium-coarse	high (164)	16	b2	a*	b1	b2_2
Aguete	3	11	medium-fine	low (60)	16	a1	b1	a	a2
	4	7.2	medium-coarse	medium (116)	52	a2*	b2_1	b3*	a1
A Cova	5	10.6	coarse	none (0)	8	b1	b2_2	b2	b1
	6	11.4	medium-coarse	none (0)	52	b1	b2_2	b2	b2_1

ES200-7C split-beam 200 kHz transducer was mounted on a steel pole attached to the hull rail of the boat. The transducer was operated with maximum emitting power (1 kW), minimum pulse length (64  $\mu$ s) and a sampling rate of 10 pings  $s^{-1}$  to obtain the maximum vertical and horizontal resolution. The acoustic survey was carried out under good weather conditions and keeping the boat's speed between 1.5 and 3.5 knots. This speed permits the oversampling of every bottom point in at least 4 consecutive pings (the split beam angle is  $7^\circ$  and the survey area depth ranges from 5–11 m), thereby ensuring spatial continuity. Positions were recorded into the sounder files using a GPS (Simrad GN33) signal input.

To define the acoustic transects, an imaginary line, parallel to the coast, was defined over each sandbar. Transects were sailed along these lines repeatedly, each one at least three times (see Figure 3, p. 507), switching the course in between, i.e. leaving the coast to the left and right sides; this was later used to assess the differences due to the ship's course. In total, 14 acoustic transects were recorded: five along the Raxó sandbar, five along Aguete and four along A Cova, with respective mean lengths of 550 m, 250 m and 285 m.

Angular information from the seabed. The phase distribution of the backscattered signal is due to the bottom surface roughness and the sub-bottom scatterers (razor shells in our study case) within the insonified seabed area.

In previous works split-beam characterisation of bottom roughness has been used to discriminate fish aggregations near the seabed (MacLennan et al. 2004) or to improve 3-D bathymetry resolution and seabed classification (Demer et al. 2009, Cutter & Demer 2010). This technique uses multifrequency transducer assemblies to overcome the baseline decorrelation problem. Our hypothesis is that a similar mechanism in the sub-bottom volume, where impedance fluctuations are due to the presence of benthic biomass, local variations of granulometry, or seabed composition, should give us angular information about the presence of razor clam patches (angle  $\varphi$  in Figure 2a and alongship and athwartship angles in Figure 2b).

In the idealised scheme of Figure 2c, the weak scatterers crossing the beam would cause variations in the echosounder angular information similar to those caused by moving point-like scatterers below the ship. In a naïve representation, as the split-beam passes by a single scatterer, the measured alongship angle will suffer a monotonous variation from positive to negative values, while the athwartship angle detected will show a more uniform value. In the case of a shellfish patch, the multiple scatterings will cause the

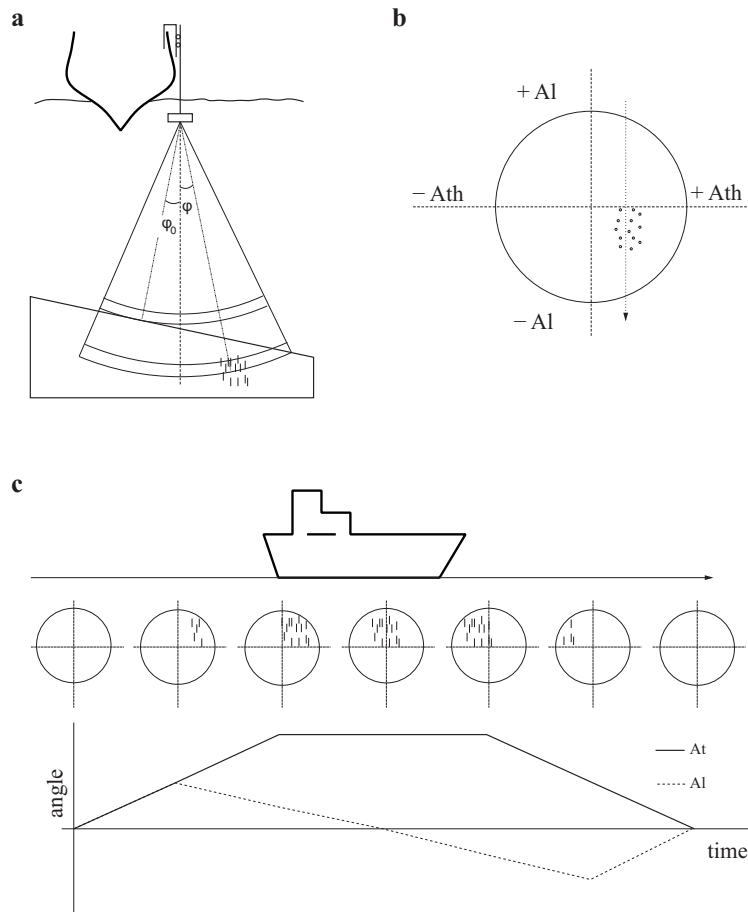


**Figure 2.** Geometry of the acquisition (a) and angles scheme (b) of the split-beam angular assignment for the case of buried scatterers in a sedimentary bottom. The expected temporal evolution of the measured angles as the transducer advances is also depicted (c)

angles (determined from the phase differences detected) to spread around the actual positions, but the time evolution of the angles will be retained.

Although their backscattered intensity is superimposed in the same way on the rest of the bottom backscatters, making them indistinguishable in the energy echogram, their angular information will compete with the interface returns and sediment volume backscatter, drawing a complex picture.

### 3. Statistical texture analysis of the echogram

The split-beam angular information was processed to provide a textural characterisation of the echogram. First-order statistics do not offer infor-

mation about variations in the angular echograms that would denote the presence of razor shells. Thus, a second-order statistical procedure, aimed at detecting correlations between neighbouring acoustic samples, should be applied in the form of a textural analysis (Haralick et al. 1973, Zaragozá et al. 2010).

The most used second-order statistic is the co-occurrence matrix, whose cell  $p_{ij}$  contains the fraction of pairs of the neighbouring signal samples (echo bins) having quantised levels  $i$  and  $j$  respectively in a preset window and after signal quantisation in  $N$  levels (Haralick et al. 1973).

The neighbouring samples of a bin can be defined in two natural ways: along the pings (being neighbours, the previous and the next bin in the same ping) or along depths (being neighbours, the bins of consecutive pings corresponding to the same depth below the detected sea bottom). We will refer to the first neighbour definition as Type 1 (or along pings) and the second one as Type 2 (or across pings). The resulting co-occurrence matrix will be symmetric as if  $i$  is followed by  $j$ , then both  $(i, j)$  and  $(j, i)$  bin pairs are counted.

Based on the co-occurrence matrices, Haralick et al. (1973) introduced the so-called textural features. Thirteen Haralick textural features (denoted as H1 to H13) have been calculated for both the alongship and athwartship angles. Another textural feature (lacunarity, Lac), describing the relationship between the co-occurrence standard deviation and the mean value, was also calculated. These variables are mathematically defined in the Appendix.

We have restricted the textural analysis to those bins contained between the bottom surface and the equivalent to 30 cm of sediment depth. This depth corresponds to the main insonified region of the echogram and also to the corer sample depth range. Four quantisation levels were defined for the angular measures scaled with the mean and standard deviation of the angle value at a given depth below the bottom. If the angle in a bin is  $\varphi$ , then the value  $\alpha = (\varphi - \bar{\varphi})/\sigma_\varphi$  is computed, where  $\bar{\varphi}$  is the mean angle and  $\sigma_\varphi$  its standard deviation in all the bins located at the same depth as the bin considered. Only those angles within two standard deviations around the mean (i.e.  $|\alpha| < 2$ ) have been taken into account in the analyses. These values were quantised to four values corresponding to the four intervals  $[-2, -1]$ ,  $[-1, 0]$ ,  $[0, 1]$  and  $[1, 2]$ .

The procedures for the echogram loading and the computation of the Haralick variables were implemented in the Octave language and are available on the website <http://www.kartenn.es/downloads>.

**Energy-based acoustic classification.** Based on the volume backscatter of the sound wave, a classification of the data could be tested using the

roughness and hardness acoustic indexes. These indexes are computed from the first and second acoustic bounces respectively, and have been introduced as seabed features (Orłowski 1982). The first echo energy (E1) is computed as the time integral of the received backscattered energy corresponding to the diffuse surface reflection (i.e. without the leading increasing power signal). The second echo energy (E2) is computed as the time integral of the entire second bounce signal. Both energies are normalised by depth applying the correction  $+20 \log(R)$ , where  $R$  is the range. This approach using two variables was introduced for seabed classification by Burns et al. (1989) and is currently used by the commercial system RoxAnn (Sonavision Limited, Aberdeen, UK).

**Multivariate statistical analysis.** The multivariate statistical method used was based on Legendre et al. (2002) and Morris & Ball (2006) and includes dimensional reduction, principal component analysis (PCA) and clustering analysis of the reduced variables. The original variables included in the analysis were the energy variables (E1, E2) and the alongship and athwartship Haralick variables, corresponding to Type 1 and Type 2 textural features. The matrix of Haralick textural features was centred and normalised and the PCA was applied (using singular value decomposition whenever more variables than samples were available) to obtain new uncorrelated variables (independent components). Only those components having eigenvalues larger than 1 were kept for the subsequent hierarchical cluster analysis (known as Kaiser's rule). This choice removes noise from the analysis retaining only variables having higher variance than the original (normalised) ones. The clustering analysis of these selected principal component variables was performed using an agglomerative nested hierarchical algorithm to generate dendrograms; complete linkage and Euclidean distances were used. Finally, a stability analysis, based on Jaccard's similarity values ( $J$ -values) was used to test the significance of these clusters, i.e. to assess how dependent was the classification obtained of the samples actually used to calculate the dendrogram. Following Henning (2008), when the  $J$ -value between two clusters found using different samples is higher than 0.75, that cluster can then be considered a valid stable cluster. The Jaccard similarity value averaged over a number of bootstrap samples will show the expected stability. All these operations were performed using the 'R' open-source statistical software (<http://www.r-project.org>).

The multivariate statistical analysis was applied to complete transects and their segments (halves, quarters and eighths of a transect) with a bottom-up scale-dependent approach in mind, addressing the spatial distribution of the substrate properties. The vessel's orientation with respect

to the coast was found to be a relevant factor for the classification; therefore all segment analyses were performed taking only transects or segments leaving the coast to port, or taking only those leaving the coast to starboard.

The results obtained from the statistical analysis of the acoustic variables were compared with the groundtruthing data from the stations (depth, sediment granulometry and razor clam and other bivalve abundance) as measured using samples taken by divers. The matching of both data sets (acoustic segments and sampling stations) was performed geographically using GIS software (ArcGis 10.0, ESRI).

#### 4. Results

Here transect and segment classifications are shown based on the acoustic analysis. The sizes of the segments, obtained by dividing each transect into equal parts, are variable. For instance, for the largest sandbar (Raxó), where the transects were around 500 m in length, the division of a transect into 4 segments provides (in the worst case) segments of about

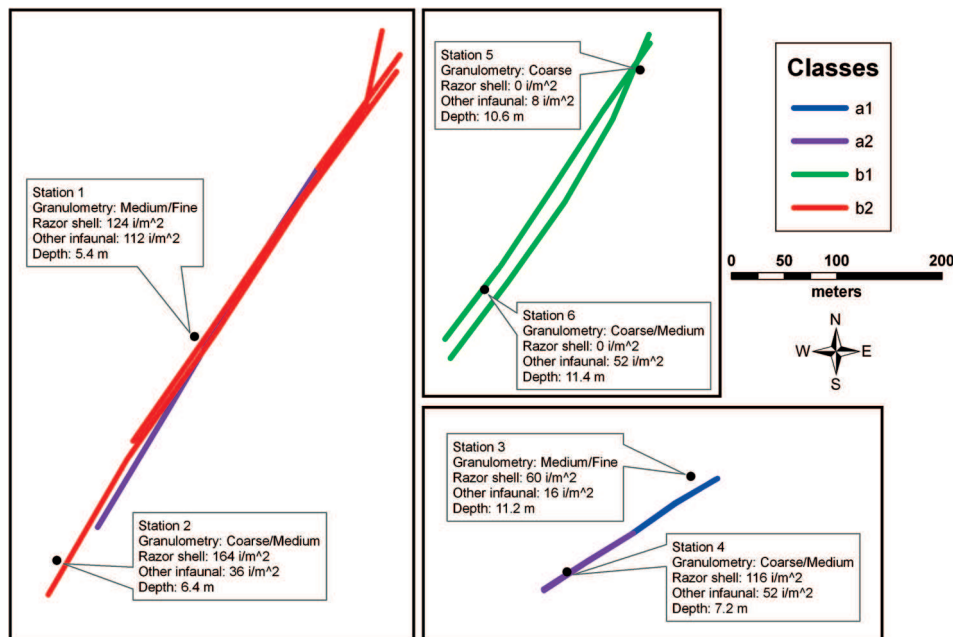


**Figure 3.** Acoustic transects over the Raxó (left), Aguete (lower right) and A Cova (upper right) beds. The colours correspond to the dendrogram branches shown in Figure 5 (Type 1 coast-to-port dendrogram). A graphical summary for each groundtruthing station is included (according to the information in Table 1)

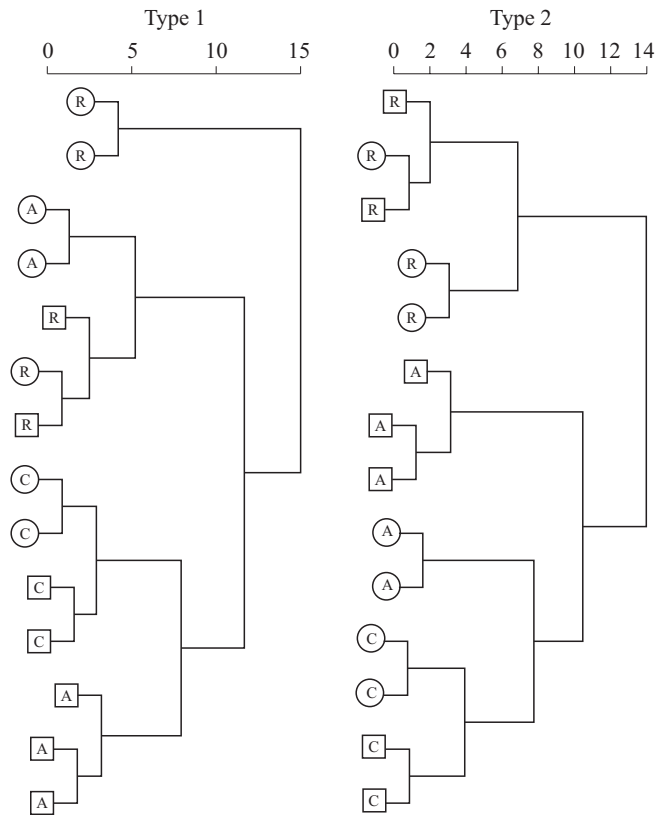


**Figure 4.** Dendrogram and classification of transects based on Type 1 (left) and Type 2 (right) features. Every leaf of the tree is labelled with the initial of the sandbar (according to Table 1) enclosed in a circle or a square, denoting that the corresponding transect was sailed leaving the coast to port or starboard, respectively

125 m; for the smaller transects of Agüete, these segments are as short as 40 m. These lengths are representative for studying the variations observed along each transect (between groundtruthing points; see Figure 3). The most relevant results are presented in Figures 3 to 6.

#### 4.1. Type 1 features

The hierarchical clustering of all the transects, based on Type 1 textural features, yields a dendrogram with three main clusters; one formed by two Raxó transects and the other two further subdivided into two sub-clusters, one corresponding to Agüete, and the others to Raxó and A Cova respectively (Figure 4). The two Agüete branches correspond to two orientations of the course: one leaving the coast to

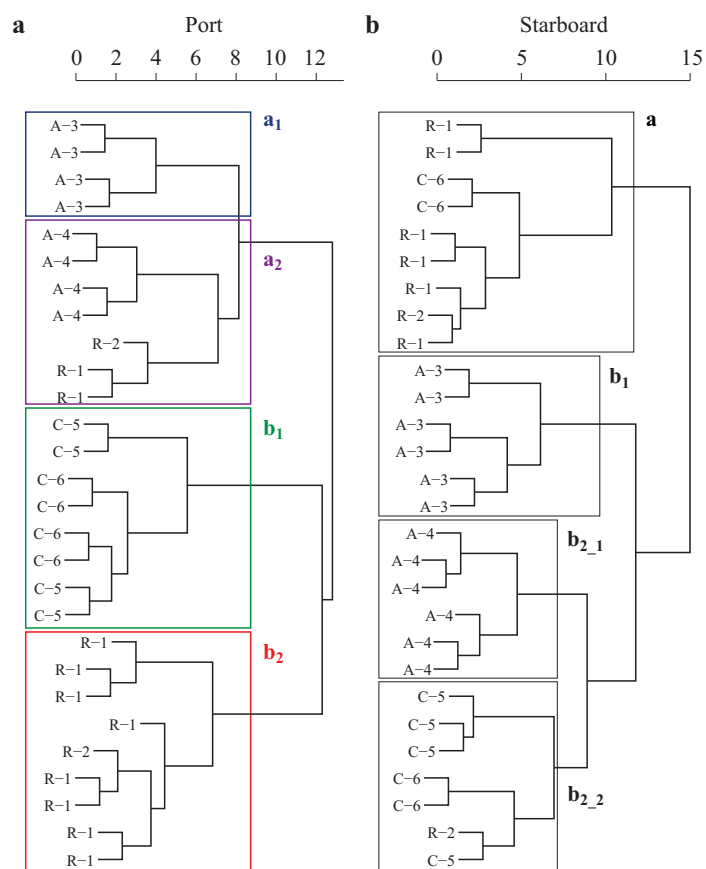


**Figure 5.** Dendrogram and classification of the segments based on Type 1 features with courses divided into a) coast-to-port and b) coast-to-starboard. Every leaf of the tree is labelled with the initial of the sandbar and the number of its nearest groundtruthing point (according to Table 1). The lower-case letters followed by numbers denote the branches and sub-branches of the dendrogram

port, the other leaving the coast to starboard. This suggests that course is a determinant variable in the classification and must be factored out to study the effect of the other variables in the classification. For this reason only the analysis of the segments taking course into account will be presented.

The PCA analysis of segment textural features shows an even distribution of the loadings of Type 1 textural features, denoting a high correlation among them. H1, H5, H9, H11 and Lac of the along-ship angular signal and H1, H3, H5, Lac of the athwartship angular signal are among the 10 most relevant ones (with higher absolute loadings, weighted by the covariance

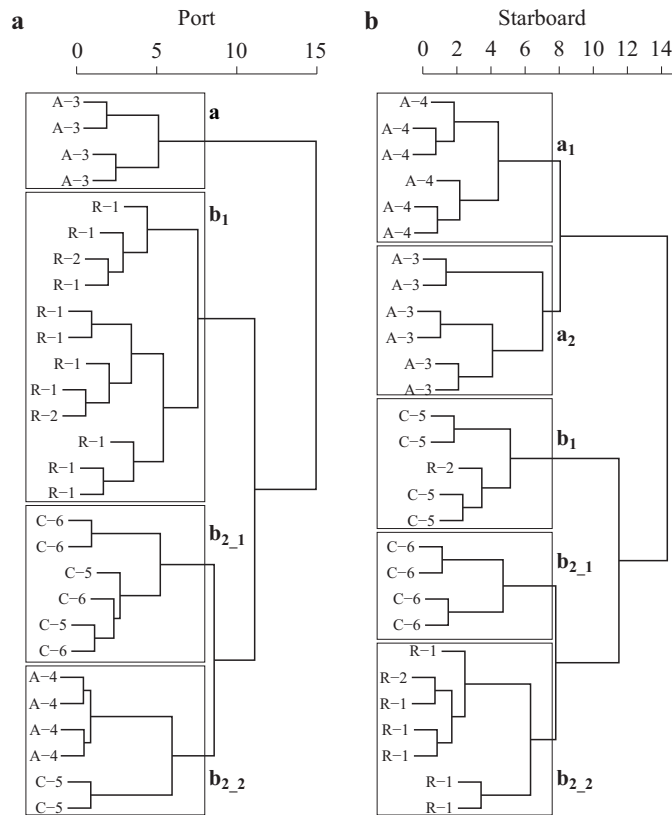


**Figure 6.** Dendrogram and classification of the segments based on Type 2 features with courses divided into a) coast-to-port and b) coast-to-starboard. Every leaf of the tree is labelled with the initial of the sandbar and the number of its nearest groundtruthing point (according to Table 1). The lower-case letters followed by numbers denote the branches and sub-branches of the dendrogram

eigenvalues) for both the coast-to-port and the coast-to-starboard groups of segments.

The hierarchical clustering of the coast-to-port segments shows four main clusters ( $a_1$ ,  $a_2$ ,  $b_1$  and  $b_2$ ), each containing segments from only one sandbar (but for  $a_2$ , see Figure 5a). The geographical distribution of this classification of coast-to-port segments can be seen in the thematic map of Figure 3. Clusters  $a_1$  and  $a_2$  (corresponding to Agute) are statistically stable: their average Jaccard indexes remain above 0.74 after resampling; the other two branches ( $b_1$  and  $b_2$ ) are very stable, with  $J$ -values above 0.90.

In the case of the coast-to-starboard transects, the four main branches of the segment dendrogram correspond to Raxó (branch  $a$ , with two misplaced

A Cova segments), another two ( $b_1$  and  $b_{2_1}$ ) to Agüete, and the last one (branch  $b_{2_2}$ ) to A Cova (with one misplaced segment from Raxó; see Figure 5b). With respect to their statistical stability, the Raxó branch, with a  $J$ -value of 0.62, is less stable, while all the others are more stable with average  $J$ -values above 0.73.

#### 4.2. Type 2 features

The hierarchical clustering of the transects based on their Type 2 textural features shows four branches: one belonging to Raxó transects, one to A Cova and the remaining two to Agüete (see Figure 4). As for Type 1 features, these results suggest that course may be a determinant variable in the classification and should be factored out prior to studying other variables.

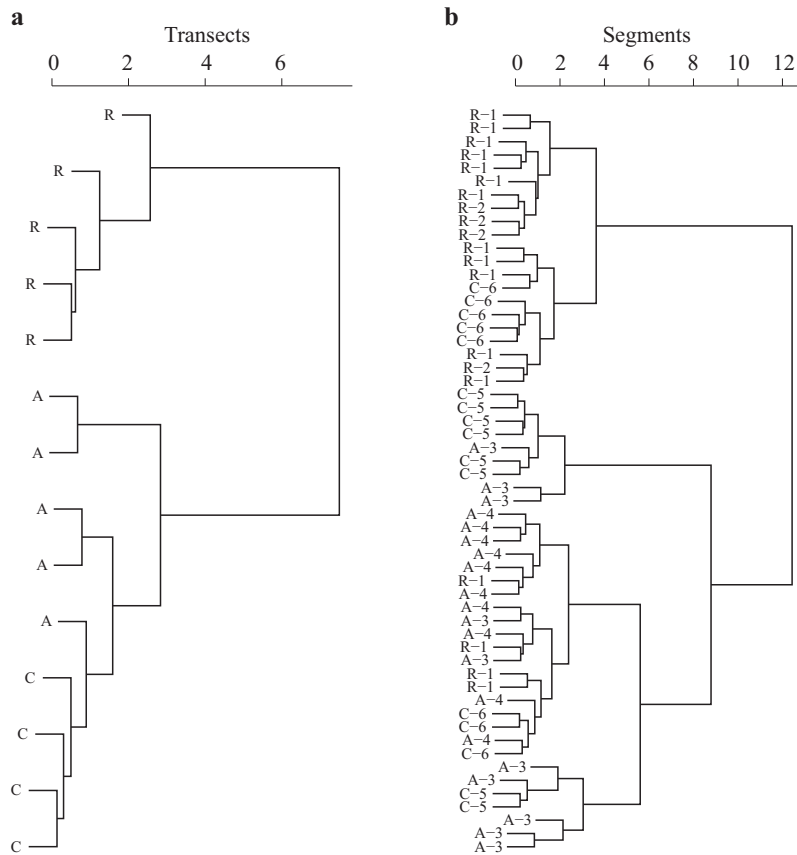
The PCA analysis again shows a balanced distribution of the loadings among the highly correlated Type 1 textural features. H1, H2, H5, H8, H9

**Table 2.** Average Jaccard indexes (measuring cluster statistical stability), estimated through bootstrap, of the classification clusters under different subsampling ratios: 1/1 (using all the pings), 1/2 (one every two pings), 1/4 and 1/8. The branch notation is the same as in Table 1 and Figures 5 and 6

Type 1									
Port clusters	Jaccard average				Starboard clusters	Jaccard average			
	1/1	1/2	1/4	1/8		1/1	1/2	1/4	1/8
$a_1$	0.74	0.73	0.88	(lost)	a	0.62	0.85	0.64	(lost)
$a_2$	0.79	0.77	0.88		$b_1$	0.73	0.52	0.52	
$b_1$	0.98	0.96	0.87		$b_{2_1}$	0.84	0.72	0.52	
$b_2$	0.92	0.78	0.99		$b_{2_2}$	0.81	0.90	0.59	

Type 2									
Port clusters	Jaccard average				Starboard clusters	Jaccard average			
	1/1	1/2	1/4	1/8		1/1	1/2	1/4	1/8
a	0.85	0.82	(lost)	(lost)	$a_1$	0.95	0.91	0.88	0.64
$b_1$	0.82	0.87			$a_2$	0.90	0.87	0.91	0.77
$b_{2_1}$	0.71	0.62			$b_1$	0.81	0.67	0.79	0.82
$b_{2_2}$	0.75	0.74			$b_{2_1}$	0.82	0.81	0.68	0.76
					$b_{2_2}$	0.80	0.78	0.76	0.76



**Figure 7.** Dendrogram and classification of transects a) and segments b) based on energy features E1 and E2

and Lac of the athwartship angular signal and H8 and Lac of the alongship angular signal are among the 10 most relevant features in both course-dependent segment classifications.

The hierarchical clustering of the coast-to-port segments keeps all of the Raxó segments in one of the four main branches (branch  $b_1$  in Figure 6a). The other branches are formed by Agüete segments (a and  $b_{2,2}$ ) and A Cova ( $b_{2,1}$ ). The average  $J$ -values of the A Cova and Agüete (close to station 3) clusters are lower, but still above 0.71, and only the other Agüete cluster attains a  $J$ -value of 0.85 corresponding to a very stable cluster.

The coast-to-starboard dendrogram (Figure 6b) groups the Agüete segments in one of the four main branches (a), with Raxó in another branch ( $b_{2,2}$ ) and A Cova split between the remaining two ( $b_1$  and  $b_{2,1}$ ). The average  $J$ -values of the two Agüete clusters (0.90 and 0.95) show them to

be very stable; but the other clusters are also stable, with average  $J$ -values above 0.80 (see Table 2).

### 4.3. Energy-based classification

The hierarchical clustering of variables E1 and E2 averaged over the transects shows a dendrogram where the Raxó transects are grouped in one of the main two branches (Figure 7a). However, the Agüete and A Cova transects appear mixed in amongst the third one; there is no clear course grouping, as in the case of angular classification. The results based on data Raxó segments remain grouped in one of the two main branches (Figure 7b). However, many segments from Agüete and A Cova are also assigned to that branch; thus the transect classification is not conserved for the segments. In the other main branch, the Agüete and A Cova segments are grouped in two sub-branches: one with most of the Agüete segments and the other of a mixed geographical origin.

## 5. Discussion

All the acoustic transects and segments covering the three sandbars in the study area have been classified using the Type 1 and Type 2 textural features, taking into account the course (leaving the coast to port or starboard).

The Agüete bed segments always show two differentiated zones, eastern and western. The other two sandbars, when divided into separate clusters in the dendrograms, do not show this spatial segregation (see the thematic map on Figure 2). This is in accordance with the razor clam density of the beds (see Table 1), which shows that Raxó and A Cova have a more even distribution than Agüete. Additionally, the distribution of the segments included in the mixed branches or the distance between neighbouring branches cannot be explained by granulometric data or razor shell density alone.

There are no a priori reasons for the asymmetry between coast-to-port and coast-to-starboard that could lead to a better classification than the one which is obtained when both courses are taken into account. Our conclusion is that this difference is probably caused by the orientation of the transducer (which was always hooked to port) with respect to the direction of the seabed maximum slope. This relative angle may affect the way the backscattered wave is reflected towards the transducer from the sea bottom and the boat hull.

Energy-based classification has been shown to be, at best, unspecific with respect to razor clam density, and our results show that the classification is worse than in the case of the angular information. Furthermore,

energy-based classification depends on the scale of analysis because segment classification shows patterns different from transect classification. In this sense the energy-based approach does not discriminate either clam densities or granulometry. For instance, all the segments of Raxó, with medium-fine and medium-coarse granulometry, are classified in a separate branch, despite the other two clam beds also having medium-coarse sand at some of their stations. An alternative hypothesis could be that energy-based classification is related to a combination of both granulometry and total bivalve density; however, not enough samples were available in this study to test this.

### 5.1. Analysis of the statistical significance of the classification methods

To assess the role of chance in the angular texture classification, the Jaccard mean values have been computed for each cluster in the dendrograms (see Table 2). According to Henning (2008), a  $J$ -value of 0.75 can be assumed to be the threshold for regarding a cluster as stable. Stable clusters are found for all Type 1 coast-to-port oriented segment classifications (except for the Agüete station 3 cluster, with a  $J$ -value of 0.73); likewise, the clusters obtained with the Type 2 textures and coast-to-starboard orientation (in fact, all of them are above 0.80) and coast-to-port orientation (except for branch b21 of A Cova, with a  $J$ -value of 0.71). These are the most statistically stable dendrograms.

Another way of assessing the statistical stability of the clusters, and thus the significance of the classification, is to test how dependent it is on the acoustic sampling conditions (given by the vessel speed and the ping rate). A numerical experiment, repeating the statistical analysis by taking one ping from every 2, 4 or 8, was performed. The results of the stability analyses are summarised in Table 2. The original labels of the dendrogram are retained, even though part of the branching structure changes (and is sometimes lost), in view of the number of segments that a cluster has in common with the original dendrogram. The Type 1 coast-to-port and the Type 2 coast-to-starboard dendrograms are the most stable under this resampling. A similar effect is observed when the segments are reduced to one eighth of a transect or less, and the number of segment mixtures increases and the cluster stability decreases. Thus, having a larger number of contiguous pings is crucial to obtaining a stable segment classification.

From the point of view of the physical information in the acoustic signal, the Type 1 features should be less affected by acquisition conditions, such as pitch and roll motions, as they are computed along single pings. Besides, the Type 2 features would capture the variations caused by the advance

of the split-beam transducer above the bottom inhomogeneities between consecutive pings.

Type 1 textures distribute segments among their corresponding sandbars, including the case when one of these sandbars is first divided into two subclusters (as in the case of Agüete, which is the one with the most heterogeneous razor clam densities). The Type 2 texture classification requires a larger number of classes to provide a classification distributing the segments among their sandbars, and also divides one of the homogeneous sandbars (A Cova) into two groups (coast-to-starboard). Thus, despite being as statistically stable as the Type 1 classification, it does not reflect as coherently the groundtruthing characteristics.

The classification groups together segments with similar razor clam densities. However, it is difficult to estimate the minimum density the method is capable of discriminating. For the surveyed razor clam beds, the most robust classifications (according to Jaccard's value criterion) can differentiate between 116 indiv.  $\text{m}^{-2}$  and 60 indiv.  $\text{m}^{-2}$  Agüete, and in most cases, between the 124 indiv.  $\text{m}^{-2}$  in Raxó and the 116 indiv.  $\text{m}^{-2}$  in Agüete. However, the method includes in the same class the 124 and the 164 indiv.  $\text{m}^{-2}$  of Raxó (probably because this last station has only two segments close to it). Given the small number of stations, the method sensitivity cannot be statistically assessed.

## 5.2. Other factors potentially affecting the classification

Energy-based methods, such as those implemented in commercial software like QTC View (Quester Tangent Corporation, Saanichton, Canada), have been found to provide classifications that are insensitive to velocity or pitch and roll motions (von Szalay & McConnaughey 2002). However, the different nature of the angular signal and the co-occurrence statistical analysis suggest the need to take vessel motion into account, for instance, to interpret the similarities between Agüete and Raxó or A Cova.

Thus, boat velocity and pitch and roll motions must be considered as potential nuisance variables in our analysis, i.e. variables potentially affecting the results, although they were not in the focus of our study. The boat velocity was recovered from the recorded GPS position and time. The pitch and roll relative time variations (the echosounder was not equipped with tilt sensors) were inferred from the variations in the acoustic reflectance around near normal insonification (where it is maximum). As the reflection coefficient near normal incidence depends strongly on angle, following the Gaussian law of width proportional to bottom roughness (Lurton 2002),

reflectance variations are expected to amplify the vessel oscillations about the vertical.

With these velocity and tilt relative variations (which, in turn, show a high degree of correlation), the same statistical analysis as for the other variables was applied. The classification results highlight the difference among the Agüete transects and the others: this is a difference not shown in the energy-based classification.

However, these results rule out these nuisance variables as the origin of bivalve clam cartography (in Figure 2). Even if the Agüete transects were different (and this caused their classification in one and the same branch), Raxó and A Cova would have been properly differentiated by the angular classification; in those cases the effect of the nuisance variables would be negligible for the relative classification.

### 5.3. Potential use of the methodology

Despite their economic importance, research efforts devoted to the cartography of infaunal bivalves are scarce. Hence, we will compare our approach with others aimed at the detection and mapping of commercial bivalve species located over the bottom surface (Kostylev et al. 2003, Hutin et al. 2005, Snellen et al. 2008). Those works used different acoustic equipment (single beam, multibeam) and their analyses were based on a classification of the energy response. The groundtruthing of Hutin et al. (2005) yielded a 71% successful classification of the clam beds, that of Snellen et al. (2008) gave between 87 and 98%. Our classification results, referred to the segments described in the previous section (spatial resolution better than 125 m), correctly assigned 93% of the segments to the right clam density class. Kostylev et al. (2003) proposed a methodology based on a multibeam echosounder that relates backscattering strength with bivalve clam density. On the basis of a regression analysis these authors conclude that the backscattering could explain 52.4% of the variability in the abundance of commercial scallops. They suggest the use of this correlation, together with a sediment type stratification, to improve scallop stock assessments in extended areas. In our case, the granulometry at the sampling stations of the three sand bars examined are sufficiently different to rule out a relationship between angular classification and granulometry. This, together with the experimental design of the transects above the sandbars of interest, is an advantage with respect to wide-area energy mapping, which requires taking the variability of geophysical features into account (Kostylev 2012).

In the present paper, angular information has been shown to be potentially useful for updating the information about the density of infaunal populations of known clam beds. Our method does not yet provide a quantitative relationship between angular features and actual individual density. Contrary to previous methods for mapping bivalve clams (lying on the sea bed), our approach is focused on clam beds with known positions. In this way, their monitoring is possible with a significantly cheaper acoustic surveying technique. Moreover, the method is well adapted to evaluate razor clam patches qualitatively, grouping them in classes of homogeneous relative density.

## 6. Conclusions

The method introduced in this paper represents a first attempt to use a split-beam echosounder for mapping and monitoring bivalve beds that lie beneath the seafloor (tens of centimetres within the sediment), as in the case of razor shells. It will be useful for mapping infaunal bivalve populations (such as the razor clam studied) that form large patches where the density varies smoothly.

We have shown that the split-beam angular signal contains relevant information about infaunal bivalve presence and density. The textural features extracted from the angular echogram successfully classified the acoustic transects (or segments of them) according to the abundance of razor clams observed in groundtruthing. The unsupervised classification is relative: points with similar razor clam densities are grouped together, although the method does not provide an absolute estimate of razor shell density. To achieve this absolute density estimation further research on the acoustic angular signal received by a split-beam echosounder from the sea bottom would be needed, but this was beyond the scope of the present work. The method improves the results based on intensity reflection, which are not sensitive enough to discriminate volume backscattering. However, it also raises new questions: Can clam patches be distinguished from a sandy seabed with subsurface coarse-grained particles? Would buried shell hash have similar signatures? Would sediment packing (as opposed to mean grain size) have an impact on the acoustic scattering? Further research should address these questions.

## Acknowledgements

We would like to thank Elena Couñago for her help in preparing the cartography and to Cristina Santa Marta and Lobo Orensanz for their careful and critical reading of the manuscript.

## References

- Adams C., Harris B., Marino II M., Stokesbury K., 2010, *Quantifying sea scallop bed diameter on Georges Bank with geostatistics*, Fish. Res., 106 (3), 460–467, <http://dx.doi.org/10.1016/j.fishres.2010.09.021>.
- Allen Y., Wilson C., Roberts H., Supan J., 2005, *High resolution mapping and classification of oyster habitats in Nearshore Louisiana using sidescan sonar*, Estuar. Coasts, 28 (3), 435–446, <http://dx.doi.org/10.1007/BF02693925>.
- Anderson J., Van Holliday D., Kloser R., Reid D., Simard Y., 2008, *Acoustic seabed classification: current practice and future directions*, ICES J. Mar. Sci., 65 (6), 1004–1011, <http://dx.doi.org/10.1093/icesjms/fsn061>.
- Bodholt H., Ness H., Solli H., 1989, *A new echo-sounder system*, Proc. Ins. Ac., 11, 123–130.
- Boswell K., Wilson M., Wilson C., 2007, *Hydroacoustics as a tool for assessing fish biomass and size distribution associated with discrete shallow water estuarine habitats in Louisiana*, Estuar. Coasts, 30 (4), 607–617.
- Burns D., Queen C., Sisk H., Mullarkey W., Chivers R., 1989, *Rapid and convenient acoustic sea-bed discrimination for fisheries applications*, Proc. Ins. Ac., 11, 169–178.
- Cutter G., Demer D., 2010, *Multifrequency biplanar interferometric imaging*, IEEE Geosci. Remote S., 7 (1), 171–175, <http://dx.doi.org/10.1109/LGRS.2009.2029533>.
- Darriba Couñago S., Fernández Tajés J., 2011, *Systematics and distribution*, [in:] *Razor clams: biology, aquaculture and fisheries*, A. Guerra Díaz, C. Lodeiros Seijo, M. Baptista Gaspar & F. da Costa González (eds.), Xunta de Galicia, Consellería do Mar, ISBN:978-84-453-4986-1.
- DeAlteris J., 1988, *The application of hydroacoustics to the mapping of subtidal oyster reefs*, J. Shellfish Res., 7, 41–45.
- Demer D., Cutter G., Renfree J., Butler J., 2009, *A statistical-spectral method for echo classification*, ICES J. Mar. Sci., 66 (6), 1081–1090, <http://dx.doi.org/10.1093/icesjms/fsp054>.
- Diaz R., Solana M., Valente R., 2004, *A review of approaches for classifying benthic habitats and evaluating habitat quality*, J. Environ. Manage., 73 (3), 165–181, <http://dx.doi.org/10.1016/j.jenvman.2004.06.004>.
- MacLennan D. N., Copland P., Armstrong E., Simmonds E., 2004, *Experiments on the discrimination of fish and sea bed echoes*, ICES J. Mar. Sci., 61 (2), 201–210, <http://dx.doi.org/10.1016/j.icesjms.2003.09.005>.
- Fismare S. L., 2011, *Avaliación da pesquería de navalla (Ensis arcuatus) da ría de Pontevedra cara unha explotación sostible: estudio e integración dos aspectos biolóxicos e hidrodinámicos na súa explotación*, Tech. Rep., Fismare Innov. Sostenibil. S. L., A Coruña, Spain.
- Folk R. L., 1954, *The distinction between grain size and mineral composition in sedimentary rock nomenclature*, J. Geol., 62 (4), 344–359, <http://dx.doi.org/10.1086/626171>.

- Foote K., 1986, *Measurement of fish target strength with a split-beam echo sounder*, J. Acoust. Soc. Am., 80, 612–621, <http://dx.doi.org/10.1121/1.394056>.
- Foote K., Kristensen F., Solli H., 1984, *Trial of a new split-beam echosounder*, Tech. Rep. Doc. 1984/B: 21, ICES.
- Grizzle R., Ward L., Adams J., Dijkstra S., Smith B., 2005, *Mapping and characterizing oyster reefs using acoustic techniques, underwater videography and quadrat counts*, Am. Fish. Soc. Symp., 41, 152–159.
- Haralick R., Shanmugam K., Dinstein I., 1973, *Textural features for image classification*, IEEE T. Syst. Man Cyb., 3(6), 610–621, <http://dx.doi.org/10.1109/TSMC.1973.4309314>.
- Hennig C., 2008, *Dissolution point and isolation robustness: robustness criteria for general cluster analysis methods*, J. Multivariate Anal., 99(6), 1154–1176, <http://dx.doi.org/10.1016/j.jmva.2007.07.002>.
- Holme N. A., 1954, *The ecology of British species of Ensis*, J. Mar. Biol. Assoc. UK, 33(1), 145–172, <http://dx.doi.org/10.1017/S0025315400003532>.
- Hutin E., Simard Y., Archambault P., 2005, *Acoustic detection of a scallop bed from a single-beam echosounder in the St. Lawrence*, ICES J. Mar. Sci., 62(5), 966–983, <http://dx.doi.org/10.1016/j.icesjms.2005.03.007>.
- Jackson D., Richardson M., 2007, *High-frequency seafloor acoustics*, Springer, New York, 616 pp.
- Jamieson G., 1993, *Marine invertebrate conservation: evaluation of fisheries over-exploitation concerns*, Am. Zool., 33(6), 551–567.
- Jamieson G., Campbell A., 1998, *Estimating king crab (Paralithodes camtschaticus) abundance from commercial catch and research survey data*, Proc. North Pacific Symp. Invertebrate Stock Assess. Manag., NRC Res. Press, 73–83.
- JiangPing T., Ye Q., XeChang T., JianBo C., 2009, *Species identification of Chinese sturgeon using acoustic descriptors and ascertaining their spatial distribution in the spawning ground of Gezhouba Dam*, Chinese Sci. Bull., 54(21), 3972–3980, <http://dx.doi.org/10.1007/s11434-009-0557-9>.
- Kostylev V. E., 2012, *Benthic habitat mapping from seabed acoustic surveys: do implicit assumptions hold?*, [in:] *Sediments, morphology and sedimentary processes on continental shelves: advances in technologies, research and applications*, M. Li, C. Sherwood & P. Hill (eds.), Wiley-Blackwell, Chichester, 405–416.
- Kostylev V. E., Courtney R. C., Robert G., Todd B. J., 2003, *Stock evaluation of giant scallop (Placopecten magellanicus) using high-resolution acoustics for seabed mapping*, Fish. Res., 60(2–3), 479–492, [http://dx.doi.org/10.1016/S0165-7836\(02\)00100-5](http://dx.doi.org/10.1016/S0165-7836(02)00100-5).
- Legendre P., Ellingsen K., Björnbohm E., Casgrain P., 2002, *Acoustic seabed classification: improved statistical method*, Can. J. Fish. Aquat. Sci., 59(7), 1085–1089, <http://dx.doi.org/10.1139/f02-096>.
- Lindenbaum C., Bennell J., Rees E., McClean D., Cook W., Wheeler A., Sanderson W., 2008, *Small-scale variation within a Modiolus modiolus*

- (*Mollusca: Bivalvia*) reef in the Irish Sea: I. Seabed mapping and reef morphology, *J. Mar. Biol. Assoc. UK*, 88 (1), 133–141, <http://dx.doi.org/10.1017/S0025315408000374>.
- Lurton X., 2002, *An introduction to underwater acoustics. Principles and applications*, Springer-Verlag, New York.
- Lyons P., 2005, *The potential impact of shell fragment distributions on high-frequency seafloor backscatter*, *IEEE J. Ocean. Eng.*, 30 (4), 843–851, <http://dx.doi.org/10.1109/JOE.2005.862082>.
- Morris L., Ball D., 2006, *Habitat suitability modeling of economically important fish species with commercial fisheries data*, *ICES J. Mar. Sci.*, 63 (9), 1590–1603, <http://dx.doi.org/10.1016/j.icesjms.2006.06.008>.
- Orłowski A., 1982, *Application of multiple echoes energy measurements for evaluation of sea bottom type*, *Oceanologia*, 19, 61–78.
- Peirson G., Frear P., 2003, *Fixed location hydroacoustic monitoring of fish populations in the tidal River Hull, north-east England, in relation to water quality*, *Fisheries. Manag. Ecol.*, 10 (1), 1–12, <http://dx.doi.org/10.1046/j.1365-2400.2003.00316.x>.
- Raineault N., Trembanis A., Miller D., 2011, *Mapping benthic habitats in Delaware Bay and the coastal Atlantic: acoustic techniques provide greater coverage and high resolution in complex, shallow-water environments*, *Estuar. Coast.*, 35 (2), 682–699, <http://dx.doi.org/10.1007/s12237-011-9457-8>.
- Rodríguez-Pérez D., Sánchez-Carnero N., Freire J., 2013, *A pulse-length correction to improve energy-based seabed classification in coastal areas*, (submitted).
- Schimmel A., Healy T., Johnson D., Immenga D., 2010, *Quantitative experimental comparison of single-beam, sidescan, and multibeam benthic habitat maps*, *ICES J. Mar. Sci.*, 67 (8), 1766–1779, <http://dx.doi.org/10.1093/icesjms/fsq102>.
- Simmonds E., MacLennan D., 2005, *Fisheries acoustics: theory and practice*, 2nd edn., Blackwell Publ., Oxford, <http://dx.doi.org/10.1002/9780470995303>.
- Snellen M., Simons D.G., Riethmueller R., 2008, *High frequency scattering measurements for mussel bed characterisation*, *Acoustics'08*, 5253–5258.
- von Szalay P.G., McConnaughey R.A., 2002, *The effect of slope and vessel speed on the performance of a single beam acoustic seabed classification system*, *Fish. Res.*, 56 (1), 99–112.
- Wildish D., Fader G., Lawton P., MacDonald A., 1998, *The acoustic detection and characteristics of sublittoral bivalve reefs in the Bay of Fundy*, *Cont. Shelf Res.*, 18 (1), 105–113, [http://dx.doi.org/10.1016/S0278-4343\(98\)80002-2](http://dx.doi.org/10.1016/S0278-4343(98)80002-2).
- Zaragozá N., Sánchez-Carnero N., Espinosa V., Freire J., 2010, *Acoustic techniques for solenoid bivalve mapping*, [in:] *Proc. Europ. Conf. Underwater Acoust.*, Vol. 1, 139–144.

---

## Appendix A

### Haralick textural variables

The textural variables introduced by Haralick et al. (1973) are defined in terms of the co-occurrence matrix cell values,  $p_{ij}$ . This set of fourteen redundant probability measures quantifies the distance of the co-occurrence matrix from that of a spatially uncorrelated signal. We have retained the order in the original paper: H1, energy or angular second moment; H2, contrast; H3, correlation; H4, variance; H5, inverse difference moment; H6, sum average; H7, sum variance; H8, sum entropy; H9, entropy; H10, difference variance; H11, difference entropy; H12, normalised relative entropy; H13, entropy angle, and H16: maximum correlation coefficient (not used in this paper). Another feature, lacunarity, describes the relationship between co-occurrence standard deviation and the mean value of  $p_{ij}$ , whereas all other Haralick variables deal with just one of them at a time. The mathematical expressions used to compute these variables are summarised in Table A.1.

**Table A.1.** Mathematical definitions of the Haralick textural variables

Energy or Angular second moment	$H_1 = \sum_{ij} p_{ij}^2$	Sum entropy	$H_8 = \sum_k p_k^+ \log \frac{1}{p_k^+}$
Contrast	$H_2 = \sum_k k^2 p_k^-$	Entropy	$H_9 = \sum_{ij} p_{ij} \log \frac{1}{p_{ij}}$
Correlation	$H_3 = \frac{1}{s^2} \sum_{ij} (i-m)(j-m)p_{ij}$	Differences variance	$H_{10} = \sum_k (k-n^-)^2 p_k^-$
Variance	$H_4 = s^2 = \sum_i (i-m)^2 p_{ix} = \sum_j (j-m)^2 p_{xj}$	Differences entropy	$H_{11} = \sum_k p_k^- \log \frac{1}{p_k^-}$
Inverse mean distance	$H_5 = \sum_{ij} \frac{p_{ij}}{1+(i-j)^2}$	Relative normalised entropy	$H_{12} = \frac{\sum_{ij} p_{ij} \log \frac{1}{p_{ij}} - \sum_{ij} p_{ij} \log \frac{1}{p_{ix}p_{xj}}}{\max \left\{ \sum_i p_{ix} \log \frac{1}{p_{ix}}, \sum_i p_{xj} \log \frac{1}{p_{xj}} \right\}}$
Sum average	$H_6 = n^+ = \sum_k kp_k^+$	Entropic angular measure	$H_{13} = \sqrt{1 - \exp \left[ -2 \sum_{ij} p_{ix}p_{xj} \log \frac{1}{p_{ix}p_{xj}} \right]}$
Sum variance	$H_7 = \sum_k (k-n^+)^2 p_k^+$	Lacunarity	$\text{Lac} = \sqrt{N \sum_{ij} p_{ij}^2 - 1}$
Auxiliary definitions			
$p_k^+ = \sum_{ i+j =k} p_{ij}$	$p_k^- = \sum_{ i-j =k} p_{ij}$	$p_{ix} = \sum_j p_{ij}$	$p_{xj} = \sum_i p_{ij}$
			$n^- = \sum_k kp_k^-$